Apoptosis induced by bruceine D in human non-small-cell lung cancer cells involves mitochondrial ROS-mediated death signaling

JIAN-HUI XIE[1*], ZHENG-QUAN LAI[2*], XING-HAN ZHENG[3], YAN-FANG XIAN[4], QIAN LI[1], SIU-PO IP[4], YOU-LIANG XIE[3], JIAN-NAN CHEN[3], ZI-REN SU[3], ZHI-XIU LIN[3] and XIAO-BO YANG[1]

[1]Guangdong Provincial Key Laboratory of Clinical Research on Traditional Chinese Medicine Syndrome, The Second Affiliated Hospital of Guangzhou University of Chinese Medicine, Guangzhou, Guangdong 510120; [2]Department of Pharmacy, Shenzhen University General Hospital, Shenzhen University, Shenzhen, Guangdong 518000; [3]Guangdong Provincial Key Laboratory of New Drug Development and Research of Chinese Medicine, Mathematical Engineering Academy of Chinese Medicine, Guangzhou University of Chinese Medicine, Guangzhou, Guangdong 510006; [4]School of Chinese Medicine, Faculty of Medicine, The Chinese University of Hong Kong, Shatin, N.T., Hong Kong, SAR 999077, P.R. China

Received January 15, 2019; Accepted August 5, 2019

DOI: 10.3892/ijmm.2019.4363

Abstract. Bruceine D is one of the active components of *Brucea javanica* (L.) Merr., which is widely used to treat cancer in China. The aim of the present study was to evaluate the potential effect of bruceine D against non-small-cell lung cancer (NSCLC) cells and delineate its underlying mechanisms. The results indicated that treatment with bruceine D markedly inhibited the proliferation of wild-type NSCLC cells and epidermal growth factor receptor-mutant cells in a dose- and time-dependent manner, and significantly decreased the colony-forming ability and migration of A549 cells. Hoechst 33342 staining and flow cytometric analysis demonstrated that treatment with bruceine D effectively induced apoptosis of A549 cells. In addition, the proapoptotic effect of bruceine D was found to be associated with G0-G1 cell cycle arrest, accumulation of intracellular reactive oxygen species (ROS) and malondialdehyde, depletion of glutathione levels and disruption of mitochondrial membrane potential. Additionally, pretreatment with N-acetylcysteine, a ROS scavenger, significantly attenuated the bruceine D-induced inhibition in A549 cells. Western blotting demonstrated that treatment with bruceine D significantly suppressed the expression of the anti-apoptotic proteins Bcl-2, Bcl-xL and X-linked inhibitor of apoptosis, enhanced the expression levels of apoptotic proteins Bax and Bak, and inhibited the expression of pro-caspase-3 and pro-caspase-8. Based on these results, it may be suggested that inhibition of A549 NSCLC cell proliferation by bruceine D is associated with the modulation of ROS-mitochondrial-mediated death signaling. This novel insight may provide further evidence to verify the anticancer efficacy of *B. javanica*, and support a role for bruceine D in the anti-NSCLC treatment.

Correspondence to: Professor Xiao-Bo Yang, Guangdong Provincial Key Laboratory of Clinical Research on Traditional Chinese Medicine Syndrome, The Second Affiliated Hospital of Guangzhou University of Chinese Medicine, 111 Dade Road, Yuexiu, Guangzhou, Guangdong 510120, P.R. China
E-mail: yangxiaobomd@163.com

Professor Zhi-Xiu Lin, Guangdong Provincial Key Laboratory of New Drug Development and Research of Chinese Medicine, Mathematical Engineering Academy of Chinese Medicine, Guangzhou University of Chinese Medicine, 232 Waihuan East Road, Guangzhou Higher Education Mega Center, Panyu, Guangzhou, Guangdong 510006, P.R. China
E-mail: linzx@gzucm.edu.cn

*Contributed equally

Key words: bruceine D, apoptosis, mitochondrial signaling pathway, reactive oxygen species, human non-small-cell lung cancer cells

Introduction

Lung cancer is a highly prevalent malignancy and the leading cause of cancer-related mortality worldwide. Non-small-cell lung cancer (NSCLC) accounts for nearly 80% of all lung cancer casesω1). Current chemotherapies have been found to be only marginally effective in prolonging overall survival. Natural products have been used as the main sources of therapeutic agents in ancient times and, in modern medicine, they remain a major source of new drug development (2,3). Isolation of anticancer compounds from traditional herbs may offer new options for lung cancer treatment.

Brucea javanica (L.) Merr. (Fructus Bruceae) and its oil emulsion have long been used for the treatment of various types of cancer in China (4). Quassinoids are characteristic metabolites of *B. javanica* and are well-known for their anticancer properties (5). Bruceine D is an abundant naturally occurring active tetracyclic triterpene quassinoid in *B. javanica*. Our previous studies have demonstrated that bruceine D exerts potent antiproliferative effects on cultured

human pancreatic adenocarcinoma cells through induction of apoptosis involving the activation of the p38-MAPK, NF-κB, and reactive oxygen species (ROS)-associated PI3K/Akt signaling pathways (6-8). By contrast, bruceine D was shown to exert only mild cytotoxic effects on human gastric mucosal epithelial GES-1 cells, human foreskin fibroblast Hs68 cells and the WRL68 human hepatocyte cell line (8-10). Furthermore, bruceine D effectively reduced the rate of xenograft human pancreatic tumor and orthotopic xenograft in nude mice, with no overt toxicity (7,8).

Although a number of studies have predominantly focused on the anti-pancreatic cancer activity of bruceine D, its potential effect and mechanism of action in other types of cancer, including lung cancer, remain elusive. As part of the ongoing investigation of natural sources of anticancer treatments, the present study was initiated to investigate the potential inhibitory effect of bruceine D on NSCLC cells *in vitro* and elucidate the underlying mechanism. In the present study, the effects of bruceine D on the proliferation of four NSCLC cell lines, including wild-type (A549 and H1650) and epidermal growth factor receptor (EGFR)-mutant (PC-9 and HCC827) cell lines, were assessed. The mechanism of action of bruceine D was also evaluated through investigation of colony formation, migratory ability, cellular apoptosis induction, cell cycle arrest, oxidative status, mitochondrial membrane potential disruption and apoptosis-associated protein expression. The aim was to investigate the cytotoxic activity and elucidate the underlying mechanism of action of bruceine D in NSCLC cells, in order to improve our understanding of the role of *B. javanica* and its commercially available derivatives in lung cancer therapy, and determine whether bruceine D may be of value as a naturally occurring candidate for the treatment of NSCLC.

Materials and methods

Plant materials and reagents. The dried ripe fruits of *B. javanica* were purchased from Zhixin Pharmaceutical Co. and were authenticated by Professor ZXL of Guangdong Provincial Key Laboratory of New Drug Development and Research of Chinese Medicine, Mathematical Engineering Academy of Chinese Medicine, Guangzhou University of Chinese Medicine, according to the methods specified in the Chinese Pharmacopoeia (11). The voucher specimen (Pan-Ca. 01) was deposited in the Herbarium of School of Chinese Medicine, The Chinese University of Hong Kong. Antibodies against procaspase-3 (cat. no. sc-7148), procaspase-8 (cat. no. sc-5263), X-linked inhibitor of apoptosis (XIAP; cat. no. sc-55550), Bcl-2 (cat. no. sc-492), Bcl-xL (cat. no. sc-8392), Bax (cat. no. sc-493), Bak (cat. no. sc-517390), β-actin (cat. no. sc-47778) and horseradish peroxidase (HRP)-conjugated secondary antibodies were purchased from Santa Cruz Biotechnology, Inc. CM-H2DCFDA (cat. no. C6827) and Rhodamine 123 (cat. no. R302) were purchased from Invitrogen; Thermo Fisher Scientific, Inc. FxCycle™ PI/RNase staining solution (cat. no. F10797) was obtained from Molecular Probes; Thermo Fisher Scientific, Inc. Dead Cell Apoptosis kit with Annexin V Alexa Fluor® 488 & Propidium Iodide (cat. no v13245) was acquired from Invitrogen; Thermo Fisher Scientific, Inc. All other chemicals were obtained from Sigma-Aldrich; Merck KGaA, unless otherwise stated.

Isolation and identification of bruceine D. Bruceine D was isolated from *B. javanica* (5 kg) in our laboratory, as described previously (12), with a yield of 1 g. Bruceine D ($C_{20}H_{26}O_9$, CAS: 21499-66-1) was obtained as a colorless amorphous solid with a melting point of 290-292˚C, in agreement with a previous report (13); UV (methanol, λmax, nm): 208, 244, 315. ESI-MS (m/z): 411.4 $[M+H]^+$, 433.4 $[M+Na]^+$, 393.5, 381.6. Nuclear magnetic resonance (NMR) spectra were recorded in CD_3OD on a Bruker AC 400 MHz FT NMR spectrometer using tetra-methylsilane as the internal standard. ^{1}H NMR (CD_3OD) δ 5.21 (s, H-1), 6.03 (m, H-3), 2.93 (d, *J*=13 Hz, H-5), 2.37 (dd, *J*=1.5 and 5 Hz, H-6), 1.83 (m, H-6), 5.09 (t, H-7), 2.32 (dt, *J*=3 and 15 Hz, H-9), 4.57 (d, *J*=5 Hz, H-11), 3.75 (d, *J*=1 Hz, H-12), 4.22 (s, H-15), 3.82 (dd, *J*=2 and 7 Hz, H-17), 4.52 (d, *J*=7 Hz, H-17), 1.96 (m, H-18), 1.41 (s, H-19), 1.17 (s, H-20). ^{13}C NMR (CD_3OD) δ 83.1 (C-1), 199.8 (C-2), 125.2 (C-3), 165.6 (C-4), 44.4 (C-5), 28.7 (C-6), 81.2 (C-7), 50.8 (C-8), 46.3 (C-9), 49.6 (C-10), 75.5 (C-11), 81.5 (C-12), 85.0 (C-13), 82.4 (C-14), 70.7 (C-15), 176.2 (C-16), 70.4 (C-17), 22.5 (C-18), 11.5 (C-19), 18.4 (C-20) (Figs. S1 and S2). The compound was identified as bruceine D by comparing its ESI-MS, ^{1}H and ^{13}C NMR spectra with the published literature (13,14). The purity of bruceine D was >98.0%, as determined by high-performance liquid chromatography with a diode-array detector (Fig. S3).

Cell lines and culture. Human NSCLC cells, including wild-type cell lines (A549 and H1650) and the EGFR-mutant PC-9 cell line, were kindly provided by the Guangdong Provincial Academy of Chinese Medical Sciences. The EGFR-mutant HCC827 cell line was obtained from the Institute of Basic Medical Sciences, Chinese Academy of Medical Sciences. All cells were maintained in RPMI-1640 medium supplemented with 10% fetal bovine serum (Gibco; Thermo Fisher Scientific, Inc.), penicillin (100 U/ml) and streptomycin (100 μg/ml) in a humidified incubator with an atmosphere of 95% air and 5% CO_2 at 37˚C.

Cell viability assay. Cell viability was assessed by the MTT assay (Invitrogen; Thermo Fisher Scientific, Inc.), as described previously (6). bruceine D was dissolved in dimethyl sulfoxide (DMSO) and stored at 2-8˚C. Culture media containing different concentrations of bruceine D (0.05, 0.5, 1, 5, 25 and 50 μg/ml) were freshly prepared at the time of each experiment. The final concentration of DMSO was <0.1% in all experiments. Cells grown in medium containing an equivalent amount of DMSO without bruceine D were used as control.

Colony formation assay. Colony formation assay was performed according to the protocol previously described, with minor modifications (15). A549 NSCLC cells were seeded in 6-well plates at a density of 200 cells per well. Different concentrations of bruceine D (1, 2.5 and 5 μg/ml) were added to the wells and incubated for 24 h. Cells were allowed to form colonies for 2 weeks post-treatment. After a 2-week incubation, all cells were fixed with 4% paraformaldehyde and stained with 0.1% crystal violet solution (Beyotime Institute of Biotechnology). After 15 min, the cells were washed with distilled water at least three times and then dried at room temperature. Images were obtained using an ordinary Nikon camera (Nikon Corporation).

Wound healing assay. A549 cells were cultured under standard conditions, as mentioned above, and plated onto 60-mm^2 dishes. Scratch wounds were created into the confluent monolayers after attaining ~90% confluence. The cell monolayer was scratched using a sterile 200-μl pipette tip and the cells were washed with PBS to remove the debris. Cells were incubated in regular culture media with 1, 2.5 and 5 μg/ml bruceine D or vehicle. Wound closure was monitored over time and photographed using an Olympus IX71 microscope (Olympus Corporation). Wound closure was quantified by measuring the remaining open area using ImageJ software, version 1.52 (National Institutes of Health). The wound open area was calculated as follows: Wound open area as percentage of original = (unmigrated area/original wound area) x100%.

Cell cycle analysis. Following incubation for 48 h, cells were harvested and fixed overnight in cold 75% ethanol at 4˚C. Next, cells were washed again with pre-cooled PBS and resuspended in 400 μl FxCycle™ PI/RNase staining solution (Molecular Probes; Thermo Fisher Scientific, Inc.), according to the manufacturer's protocol. The samples were incubated for 30 min at room temperature in the dark, and then analyzed using a CytomicsTM FC500 flow cytometer (Beckman Coulter, Inc.). Cell cycle distribution was calculated with ModFit LT 4.1 software (Becton Dickinson and Company).

Annexin V-PI staining apoptosis assay. A549 cells were seeded onto 6-well plates at a seeding density of $5x10^5$ cells/well and allowed to adhere overnight. Bruceine D was added to the culture media to the specified final concentrations (1, 2.5 and 5 μg/ml). Vehicle alone was added to the culture medium, serving as the untreated control. After 48 h, the cells were harvested, rinsed twice with 1X PBS, and resuspended in 100 μl 1X Annexin binding buffer. Apoptosis was analyzed by flow cytometry (Beckman Coulter, Inc.) using Dead Cell Apoptosis kit with Annexin V Alexa Fluor® 488 & Propidium Iodide (Invitrogen; Thermo Fisher Scientific, Inc.) according to the manufacturer's instructions. Fluorescence minus one controls were used to set the positive/negative cell gates and validate the flow cytometric results.

Measurement of ROS. The ROS level was measured using the CM-H2DCFDA probe (Invitrogen; Thermo Fisher Scientific, Inc.), according to the manufacturer's protocol, followed by analysis using CXP cytometer software (version 2.0) and a flow cytometer (Beckman Coulter, Inc.).

To eliminate ROS generation, N-acetylcysteine (NAC; 20 μM) was dissolved in PBS and incubated with the cells 1 h prior to bruceine D treatment. A549 cells were treated with vehicle, 20 μM NAC, 20 μM NAC + 5 μg/ml bruceine D, or 5 μg/ml bruceine D for 48 h at 37˚C in 96-well microplates. Cell viability was assessed by the MTT assay, as described above.

Glutathione (GSH) and malondialdehyde (MDA) assays. Following treatment, A549 cells were washed twice with ice-cold PBS, harvested by centrifugation at 1,000 x g for 4 min at 4˚C, pooled in 0.5 ml PBS and homogenized. The homogenate was centrifuged at 4,000 x g for 15 min at 4˚C, and the supernatant was collected for GSH and MDA assays.

GSH content was measured as previously described (16). The GSH level was normalized to the protein concentration of each sample and expressed as fold change compared with the control group.

The MDA content was determined using the thiobarbituric acid method, as previously described (16). The MDA level was normalized to the protein concentration of each sample and expressed as fold change compared with the control group.

Measurement of mitochondrial membrane potential ($\Delta\Psi m$). The $\Delta\Psi m$ of cells exposed to 1, 2.5 and 5 μg/ml bruceine D or vehicle alone was measured using the fluorescent cationic dye Rhodamine 123, according to the manufacturer's protocol (Molecular Probes; Thermo Fisher Scientific, Inc.). Cells were analyzed using a CytomicsTM FC500 flow cytometer (Beckman Coulter, Inc.).

Western blotting. A549 cells were seeded in culture dishes (100 mm^2; $5x10^6$ cells/dish) and treated with bruceine D (1, 2.5 and 5 μg/ml) for 24 h at 37˚C after seeding. The cells were lysed with RIPA buffer containing protease inhibitor cocktail (Roche Molecular Biochemicals), 1 mM PMSF and 1 mM Na_3NO_4. The protein concentration was determined by the BCA assay (BCA kit; Sigma-Aldrich; Merck KGaA). Protein aliquots (50-μg) were placed in each lane, separated by 10% SDS-PAGE and electrotransferred to a PVDF membrane (EMD Millipore). After four washes, the membranes were incubated with 5% skimmed milk for 2 h at room temperature, and then incubated overnight at 4˚C with primary antibodies (1:200, Santa Cruz Biotechnology, Inc.) against Bax, Bad, Bcl-2, Bcl-xL, X-linked inhibitor of apoptosis (XIAP), pro-caspase-3 and pro-caspase-8. After washing three times with TBST (0.1% v/v Tween-20 in TBS), the membranes were incubated for 2 h at room temperature with species-specific HRP-conjugated secondary antibodies (1:2,000; Santa Cruz Biotechnology, Inc.) for 1.5 h. Immunoreactive bands were visualized using the ECL chemiluminescent substrate reagent kit (NOVEX). β-actin (1:500, Santa Cruz Biotechnology, Inc.) served as the loading control. ImageJ software, version 1.52 (National Institutes of Health) was used to quantify the intensity of the immunoreactive bands.

Statistical analysis. Data are presented as the mean ± standard error of the mean. The experiments were repeated three times. Multiple-group comparisons were performed using one-way analysis of variance followed by Fisher's least significant difference test to detect differences between treatment groups and the control. $P<0.05$ was considered to indicate a statistically significant difference. All statistical tests were performed using SPSS software, version 17.0 (SPSS, Inc.).

Results

Bruceine D inhibits the proliferation of wild-type and EGFR-mutant NSCLC cells. To evaluate the effect of bruceine D on the viability of NSCLC cells, wild-type A549 and H1650 cells, and EGFR-mutant PC-9 and HCC827 cells were treated with various concentrations of bruceine D (0, 0.05, 0.5, 5, 25 and 50 μg/ml) for different time periods (24, 48 and 72 h), and the cell viability was evaluated by

the MTT assay. The results revealed that bruceine D treatment inhibited the proliferation of the four NSCLC cells in a concentration- and time-dependent manner (Fig. 1B). Following treatment with bruceine D for 72 h, the IC_{50} values were 1.01±0.11, 1.19±0.07, 2.28±1.54 and 6.09±1.83 μg/ml for A549, H1650, PC-9 and HCC827 cells, respectively. In addition, the IC_{50} values were 2.26±0.48, 1.76±0.15, 1.14±0.03 and 3.48±0.10 μg/ml for cisplatin in A549, H1650, PC-9 and HCC827 cells, respectively (Fig. 1C). These results indicated that bruceine D exerted either a similar or superior anti-NSCLC effect compared with cisplatin.

Bruceine D inhibits colony formation and migration of A549 NSCLC cells. Considering that bruceine D exhibited potent cytotoxic activity against A549 cells, this cell line was used in the subsequent experiments. To investigate the inhibitory potential of bruceine D on the colony-forming ability of A549 NSCLC cells, a colony formation assay was performed. As shown in Fig. 2A, the number of colonies makedly decreased in a dose-dependent manner following treatment with bruceine D, suggesting that bruceine D exerts an anti-colony forming effect on A549 cells. This result was consistent with the results of the MTT assay, indicating that bruceine D exhibits antiproliferative activity against A549 cells.

To elucidate the potential anti-migratory effect of bruceine D on A549 cells, a would healing assay was performed. As shown in Fig. 2B, bruceine D-treated cells migrated at a slower rate compared with the control group in a time- and dose-dependent manner, indicating that bruceine D exerts a potent suppressive effect on A549 cell migration.

Bruceine D increases apoptosis of A549 NSCLC cells. To further verify whether decreased viability was associated with an induction of apoptosis, flow cytometric analysis was performed. As shown in Fig. 3A, bruceine D treatment induced early and late apoptosis in a concentration-dependent manner compared with the untreated control cells. In the untreated group there was a small percentage (0.44±0.05%) of Annexin V-positive cells. By contrast, the percentage of apoptotic cells significantly increased to 12.5±0.28, 21.58±0.50 and 25.98±0.44% (all $P<0.01$) in a concentration-dependent manner following treatment with bruceine D (1, 2.5 and 5 μg/ml, respectively) (Fig. 3B). These results suggest that the reduction in the viability of A549 cells is associated with apoptosis induced by bruceine D.

Bruceine D induces G0/G1 phase cell cycle arrest in A549 cells. Cell cycle regulation is a critical event in cellular division and is considered a valuable target in anticancer therapies (17). To investigate the potential mechanism underlying the antiproliferative activity of bruceine D, flow cytometry was used to determine the cell cycle distribution. As shown in Fig. 4, bruceine D at 1, 2.5 and 5 μg/ml significantly increased the percentage of cells in the G0/G1 phase (all $P<0.01$) and significantly decreased the ratio of cells in the S phase ($P>0.05$, $P<0.05$ and $P<0.01$, respectively). However, the percentage of cells in the G2/M phase remained almost unchanged following bruceine D treatment. These results indicated that bruceine D may inhibit the proliferation of A549 cells, at least partially by inducing cell cycle arrest at the G0/G1 phase.

Bruceine D induces ROS overproduction, GSH depletion and MDA accumulation in A549 cells. Redox disequilibrium has been reported to play a pivotal role in apoptosis (18). To investigate whether ROS generation is involved in bruceine D-induced apoptosis of A549 cells, the fluorescence probe DCFH-DA was used to measure the intracellular ROS levels. As shown in Fig. 5A, flow cytometry revealed that bruceine D markedly induced ROS generation in A549 cells. After treatment with 1, 2.5 and 5 μg/ml bruceine D, the level of intracellular ROS significantly and dose-dependently increased from 100±5.36 to 156.18±6.83, 202.11±9.43 and 251.90±4.55%, respectively (all $P<0.01$; Fig. 5B).

To verify whether ROS generation is associated with the bruceine D-induced inhibition, cells were treated with bruceine D in the presence or absence of NAC, a typical ROS scavenger. It was observed that the cell survival rate was significantly increased by NAC pre-treatment compared with that of cells subjected to bruceine D treatment alone ($P<0.05$; Fig. 5C). This result further confirms that the accumulation of ROS is involved in the suppressive effect of bruceine D on A549 cells.

As shown in Fig. 5D, the GSH level significantly decreased following bruceine D treatment, from 100±0.07 at 0 μg/ml to 67.9±2.49, 39.7±1.67 and 22.0±0.01% at 1, 2.5 and 5 μg/ml, respectively (all $P<0.01$). By contrast, the cellular MDA levels in the 1, 2.5 and 5 μg/ml bruceine D treatment groups were significantly higher compared with the control group (2.6-, 3.7- and 4.1-fold, respectively; all $P<0.01$; Fig. 5E). These findings indicate that a redox disequilibrium may contribute to the bruceine D-induced apoptosis of A549 NSCLC cells.

Bruceine D decreases the $\Delta\psi$m and triggers the mitochondrial signaling pathway in A549 cells. Mitochondria play a key role in the regulation of ROS and apoptosis, and alternations in the $\Delta\psi$m may reflect mitochondrial dysfunction, redox status imbalance and apoptotic events (19). Therefore, in the present study, the $\Delta\psi$m was detected in A549 cells by flow cytometry following staining with Rhodamine 123 (Fig. 6A and B). The results revealed that, following treatment with bruceine D (1, 2.5 and 5 μg/ml), the mean fluorescence intensity of Rhodamine 123 significantly decreased from 100±3.74 to 70.13±0.88, 62.23±1.48 and 50.33±1.97%, respectively (all $P<0.01$; Fig. 6B). These data indicate that apoptosis induced by bruceine D is associated with an alteration of the $\Delta\psi$m.

The Bcl-2 family, which includes both anti- and proapoptotic members, constitutes a key checkpoint in the intrinsic mitochondrial pathway of apoptosis (20). To investigate whether mitochondrial apoptotic events are involved in bruceine D-induced apoptosis, the present study analyzed changes in the levels of Bcl-2 family proteins and XIAP. As shown in Fig. 6C, bruceine D significantly downregulated the expression levels of Bcl-2, Bcl-xL and XIAP, and markedly upregulated the expression levels of Bax and Bak in A549 cells. Therefore, changes in the expression levels of Bcl-2 family proteins and XIAP in A549 cells may play an important role in bruceine D-induced apoptosis.

The sequential activation of caspases is a key step in the execution phase of cell apoptosis. Pro-caspase-3 and its activator, pro-caspase-8, are two important executioners of apoptosis in the extrinsic pathway, and their inhibition may

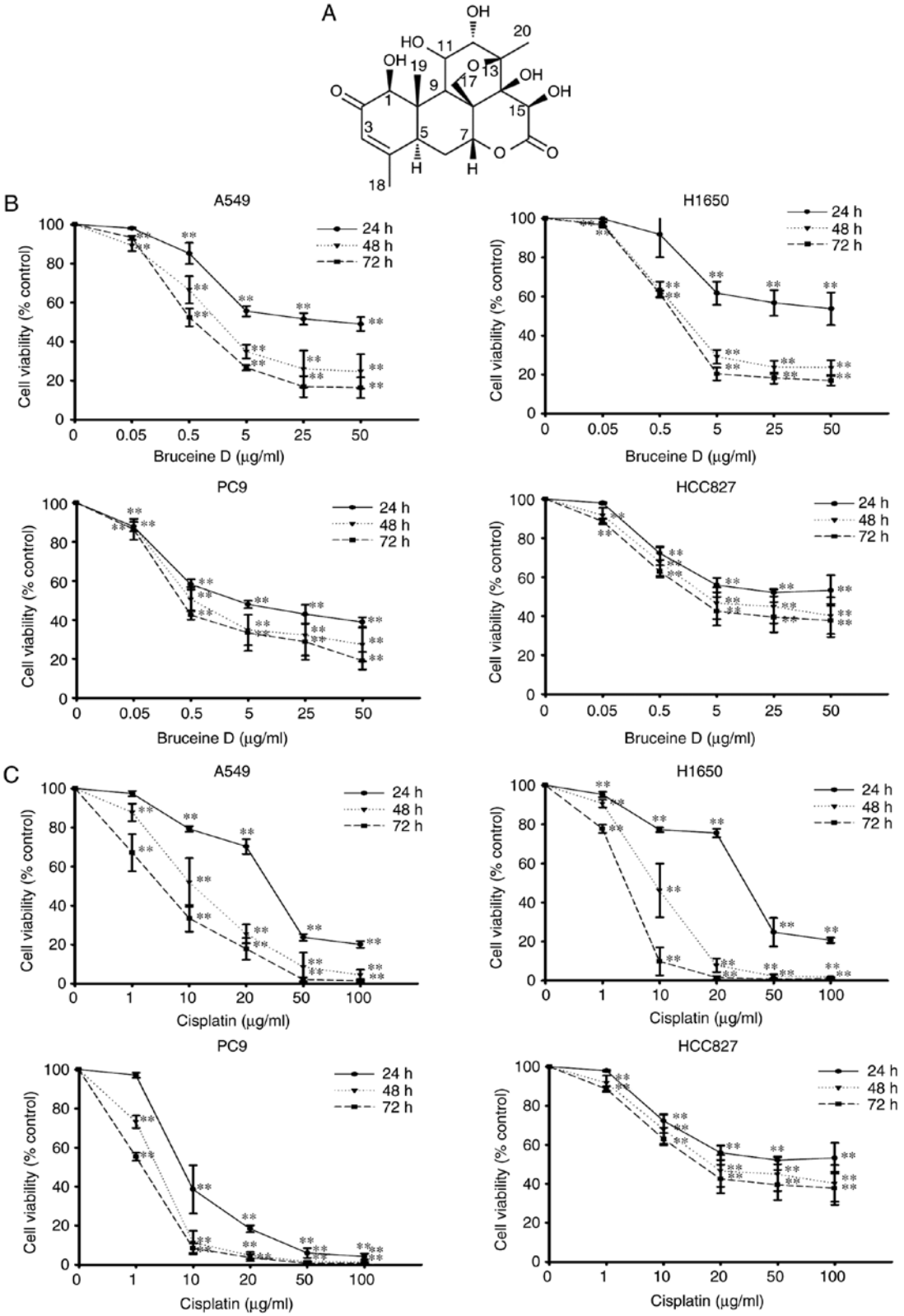

Figure 1. Antiproliferative effects of bruceine D on four NSCLC cell lines. (A) The chemical structure of bruceine D is characterized by a pentacyclic C-20 picrasane framework and a methyleneoxy bridge between C-8 and C-13. (B and C) Dose- and time-dependent antiproliferative effects of bruceine D and cisplatin on A549, PC9, H1650 and HCC827 cells. Data are presented as the mean ± standard error of the mean of three independent experiments. **P<0.01 compared with the control group (untreated cells). NSCLC, non-small-cell lung cancer.

play a key role in inducing apoptosis (21). Therefore, the role of pro-caspase-3 and pro-caspase-8 in bruceine D-induced A549 apoptosis was investigated by western blotting. The results demonstrated that bruceine D markedly downregulated the expression of pro-caspase-3 and pro-caspase-8 in a dose-dependent manner. These results suggest that the caspase family may be involved in bruceine D-induced apoptosis of A549 cells.

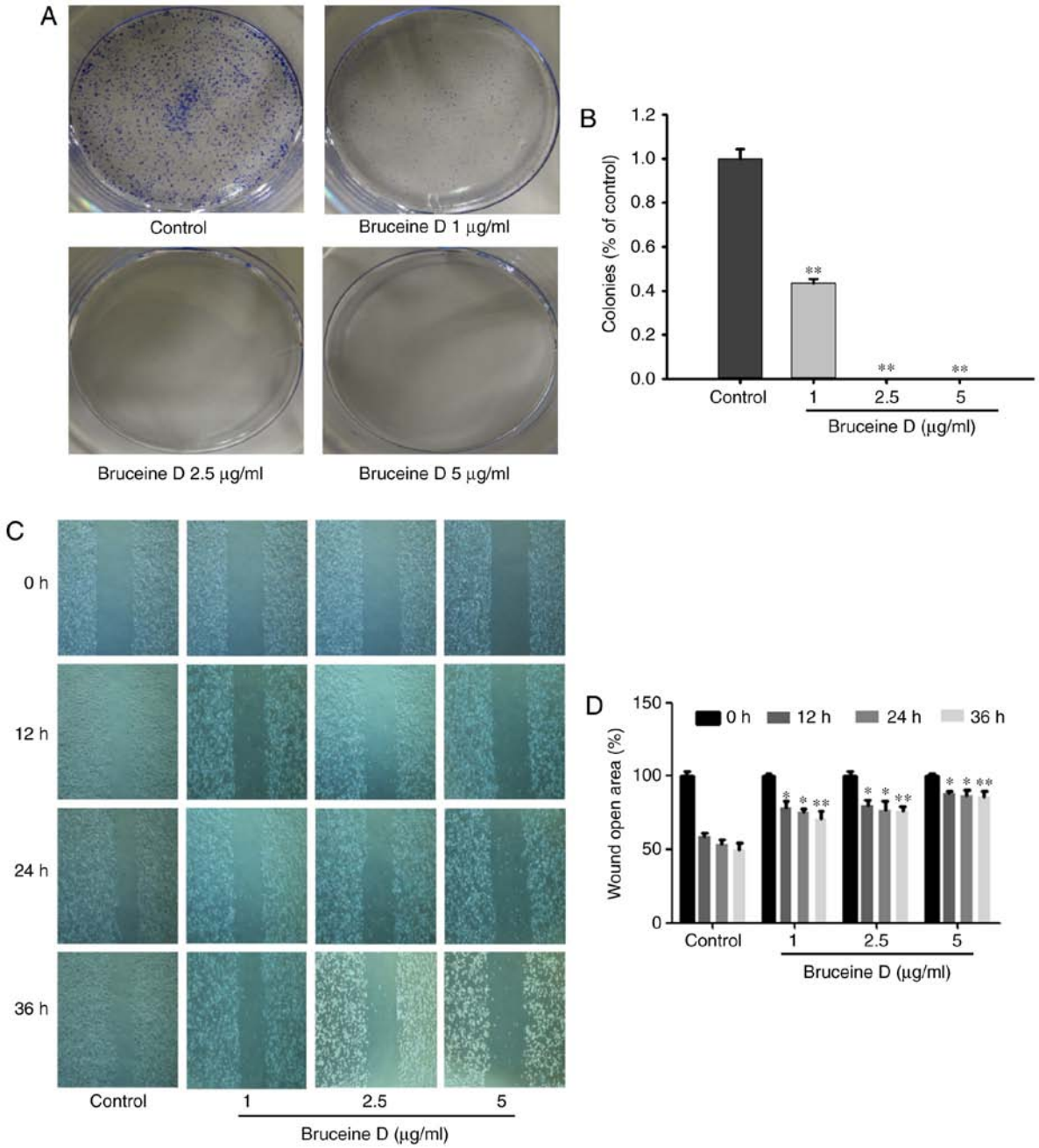

Figure 2. Inhibition of colony formation and cell migration by bruceine D. (A) Representative image of the colony formation assay. (B) Quantitative analysis of the anticlonogenic effect. (C) Representative images of the wound healing assay (magnification, x100). Images were captured at 0, 12, 24 and 36 h after scratching. (D) Quantitative result of the anti-migratory effect of bruceine D. Data are presented as the mean ± standard error of the mean of three independent experiments. Statistical analyses were performed using Fisher's least significant difference test. *P<0.05 and **P<0.01 vs. control of the corresponding time point.

Discussion

Quassinoids, a family of molecules with potent anticancer properties, have been established as the major category of anticancer phytochemicals of *B. javanica*, which is commonly used for the treatment of cancer in Southeast Asia (4). bruceine D, one of the major active quassinoids isolated from *B. javanica*, has been reported to exert an inhibitory effect against several types of cancer (8,22,23). In our previous research, bruceine D was found to exhibit a prominent suppressive effect on the proliferation of various pancreatic cancer cells, displaying only modest cytotoxicity against normal tissue cell lines, including GES-1 cells, human pancreatic progenitor cells and the WRL68 human hepatocyte cell line (6,8-10). Furthermore, bruceine D administration at a high dose (3 mg/kg) was associated with no obvious toxicity or distant organ metastasis in mice (8). Therefore, this naturally occurring tetracyclic triterpene quassinoid is considered to be promising and may be further developed into an effective and less toxic candidate for the treatment of cancer. In the present study, it was demonstrated that bruceine D-induced inhibition of NSCLC A549 cells was associated with reduced migration and colony formation, increased apoptosis, induced G0/G1 cell cycle arrest, and a disruption of the intracellular redox equilibrium and $\Delta\psi$m. bruceine D induced pro-apoptotic signaling at least partially via triggering the mitochondrial ROS-mediated death signaling pathway.

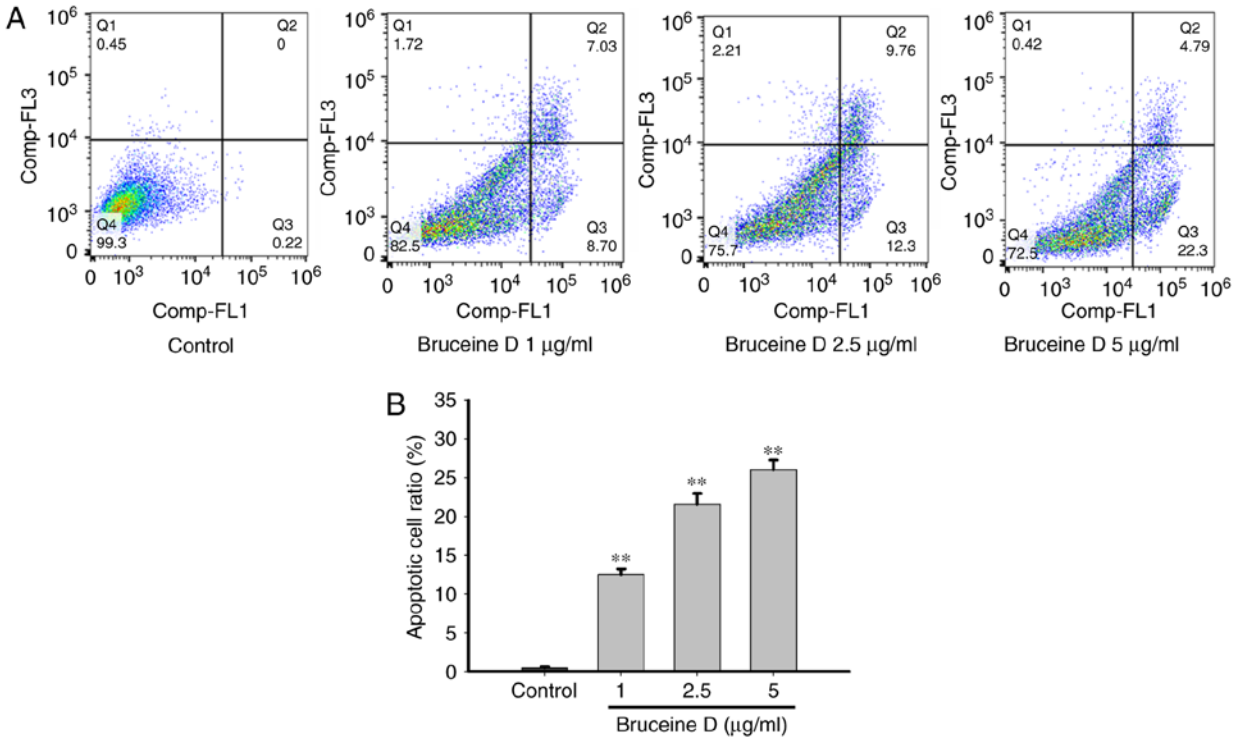

Figure 3. Bruceine D promotes apoptosis of A549 cells. (A) Representative flow cytometric analysis. (B) Quantitative analysis of the apoptotic rates. Dot plots represent the four different cell populations. The Annexin V-FITC$^-$/PI$^-$ cell population is considered as normal, the Annexin V-FITC$^-$/PI$^+$ population indicates cell necrosis, and the Annexin V-FITC$^+$/PI$^-$ and Annexin V-FITC$^+$/PI$^+$ cell populations are considered to be early and late apoptotic cells, respectively. Data are presented as the mean ± standard error of the mean of three independent experiments. Statistical analyses were performed using Fisher's least significant difference test. **P<0.01 vs. control. PI, propidium iodide.

Migration is a key characteristic of cancer progression and metastasis (24), and suppression of cancer cell migration ability may be an effective mechanism for arresting cancer metastasis. Therefore, the present study evaluated the effect of bruceine D on the migratory ability of A549 cells. A wound healing assay revealed that bruceine D significantly and dose-dependently reduced the migration of A549 cells. Furthermore, the anticlonogenic effects of bruceine D were evaluated, and bruceine D was shown to significantly inhibit colony formation by decreasing the number and size of colonies of A549 cells. In summary, these results indicate that bruceine D exerts both anti-migratory and anticlonogenic effects on A549 NSCLC cells.

Apoptosis plays a key role in cell proliferation, differentiation, senescence and death (25). Therefore, the ability to induce cancer cell apoptosis has been established as a valuable anticancer strategy. Bruceine D was previously found to exert potent apoptotic effects on hepatocellular carcinoma (22), pancreatic adenocarcinoma (8) and human chronic myeloid leukemia K562 cells (23). Using fluorescence microscopy and an Annexin V-FITC assay, the present study demonstrated that bruceine D induces apoptosis of A549 NSCLC cells. Following bruceine D exposure, the viability of A549 cells decreased rapidly, and the majority of the cells were shrunken and detached from the substratum of the culture dish (Data S1 and Fig. S4A). Typical apoptotic morphological changes, including condensation of chromatin, nuclear fragmentation and apoptotic bodies, were observed in bruceine D-treated A549 cells (Data S1 and Fig. S4B). Flow cytometric analysis indicated that bruceine D treatment significantly induces both early and late apoptosis in A549 cells, confirming that bruceine D is an effective inducer of apoptosis in A549 cells.

Cell cycle regulation has been hypothesised to be a critical step in cancer chemoprevention (26) and is considered as a feasible strategy for slowing tumor growth (17). Following bruceine D treatment, G0/G1 cell cycle arrest was observed. In addition, the proportion of cells in the S phase was significantly decreased, which indicates inhibition of DNA synthesis. By contrast, the proportion of cells in the G2/M phase was less affected. Therefore, treatment of A549 cells with bruceine D inhibited the cell cycle transition from the G1 to the S phase, suggesting that inhibition of cell cycle progression may be one of the mechanisms through which bruceine D inhibits the proliferation of A549 NSCLC cells. The present results are consistent with those of previous studies demonstrating that bruceine D induces G1 phase arrest in cancer cell lines (6,10).

The generation of intracellular ROS and depletion of GSH are closely associated with cellular apoptosis and disruption of the $\Delta\psi$m (18). ROS are vital for cell proliferation, differentiation, apoptosis and survival (27). ROS at low concentrations are crucial for maintaining redox equilibrium and cell proliferation (28). However, overaccumulation of intracellular ROS leads to mitochondrial dysfunction, which may reciprocally increase ROS production, leading to oxidative stress, lipid peroxidation, depletion of GSH and consequent cell apoptosis or death (17). GSH is a major non-enzymatic antioxidant that participates in the maintenance of the cellular redox status (29). Low GSH levels are associated with mitochondrial dysfunction and induction of apoptosis, thereby increasing sensitivity to anticancer drugs (30). The level of MDA, an intermediate

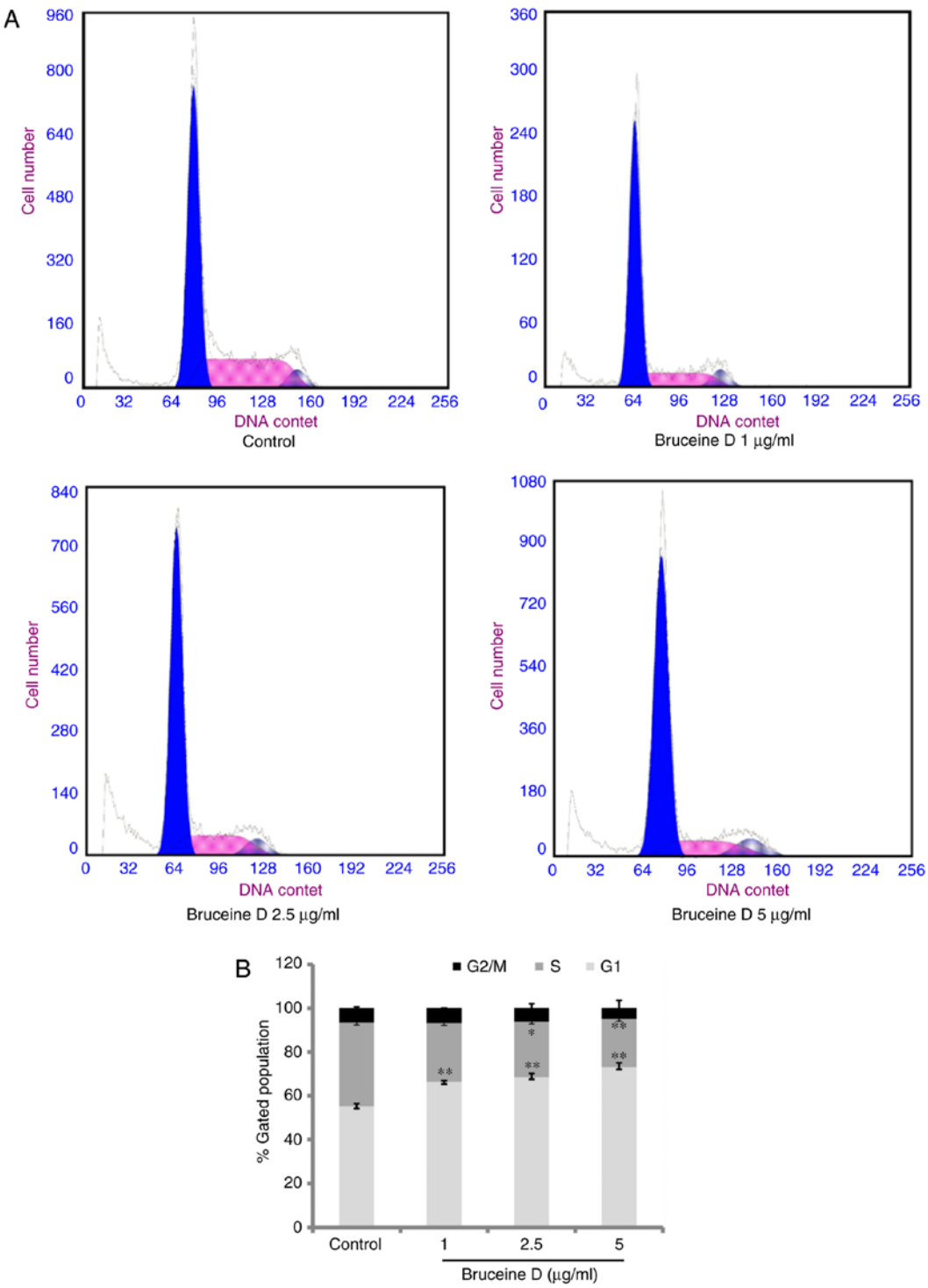

Figure 4. Bruceine D leads to G0/G1 cell cycle arrest of A549 NSCLC cells. (A) Representative flow cytometric analysis. (B) Quantitative results. Data are presented as the mean ± standard error of the mean of three independent experiments. Statistical analyses were performed using Fisher's least significant difference test. *P<0.05, **P<0.01 vs. control. PI, propidium iodide; NSCLC, non-small-cell lung cancer.

product of lipid peroxidation, directly reflects the oxidative damage of cell membranes. In the present study, increased intracellular ROS and MDA levels associated with depleted GSH levels were observed in bruceine D-treated A549 cells. Furthermore, the inhibitory effect was significantly reversed by pretreating the cells with the ROS scavenger NAC prior to bruceine D treatment, suggesting that oxidative stress caused by ROS accumulation is involved in the anti-NSCLC effect of bruceine D. These results suggest that bruceine D-induced overproduction of ROS and redox disequilibrium may play a key role in the inhibition of A549 cells.

Mitochondria play an important role in the alteration of the intracellular redox state and induction of apoptosis (31). Disruption of $\Delta\psi m$ is an initial and irreversible step of apoptosis. Mitochondrial dysfunction resulting from a decrease of $\Delta\psi m$ may cause defects in ROS production and lipid homeostasis, leading to DNA damage and apoptosis (32). In the present study, when A549 cells were exposed to bruceine D, a change

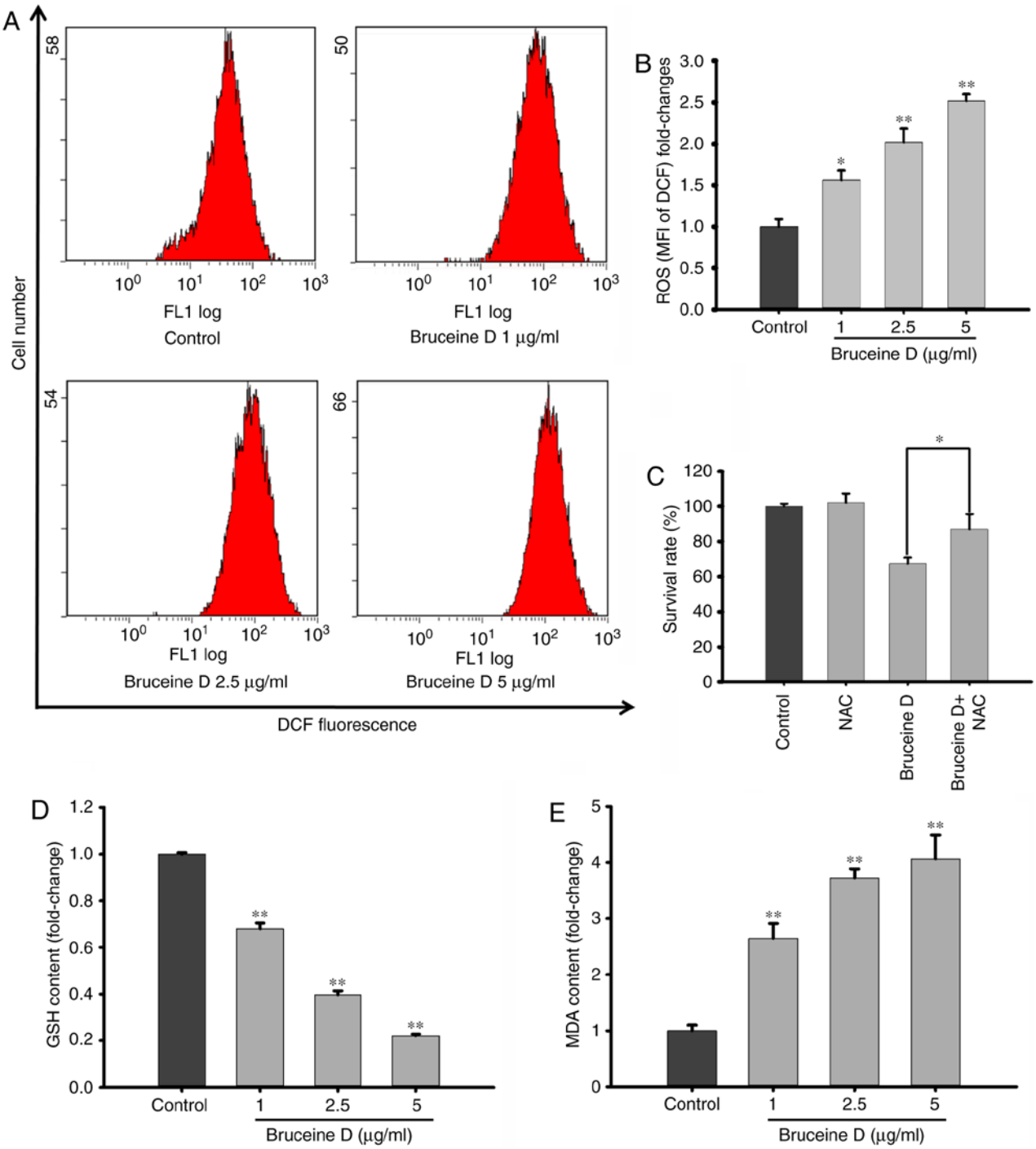

Figure 5. Effects of Bruceine D on ROS, GSH and MDA levels. (A) Representative flow cytometric analysis of ROS as estimated by CM-H2DCFDA fluorescence levels. (B) Column bar graph of cell fluorescence for CM-H2DCFDA. (C) Cell pre-treatment with NAC attenuated the bruceine D-induced inhibition. (D) GSH depletion was observed in bruceine D-induced A549 cells. (E) MDA accumulation was identified in A549 cells treated with bruceine D. Data are presented as the mean ± standard error of the mean of three independent experiments. Statistical analyses were performed using Fisher's least significant difference test. *P<0.05, **P<0.01 vs. control. ROS, reactive oxygen species; GSH, glutathione; MDA, malondialdehyde.

in Δψm was detected, indicating that mitochondrial dysfunction contributes to the anti-NSCLC effect of bruceine D.

Apoptosis usually occurs via the mitochondrial intrinsic pathway and/or the death receptor extrinsic pathway (33). The intrinsic pathway of apoptosis is regulated by the Bcl-2 family of proteins (34). Anti-apoptotic proteins, including Bcl-2 and Bcl-xL, and pro-apoptotic proteins, including Bad, Bax and Bak, which exert opposing effects on mitochondria, are two subgroups of the Bcl-2 family (35). Enhancement of pro-apoptotic protein expression compared with anti-apoptotic proteins may increase the permeability of the mitochondrial membrane, which in turn results in the release of apoptogenic factors (36). In the present study, bruceine D treatment substantially downregulated the expression of Bcl-2 and Bcl-xL, whereas it markedly upregulated the expression levels of Bad, Bax and Bak, resulting in of A549 cell apoptosis. These experimental findings suggest that bruceine D-induced apoptosis is associated with the regulation of the mitochondrial pathway.

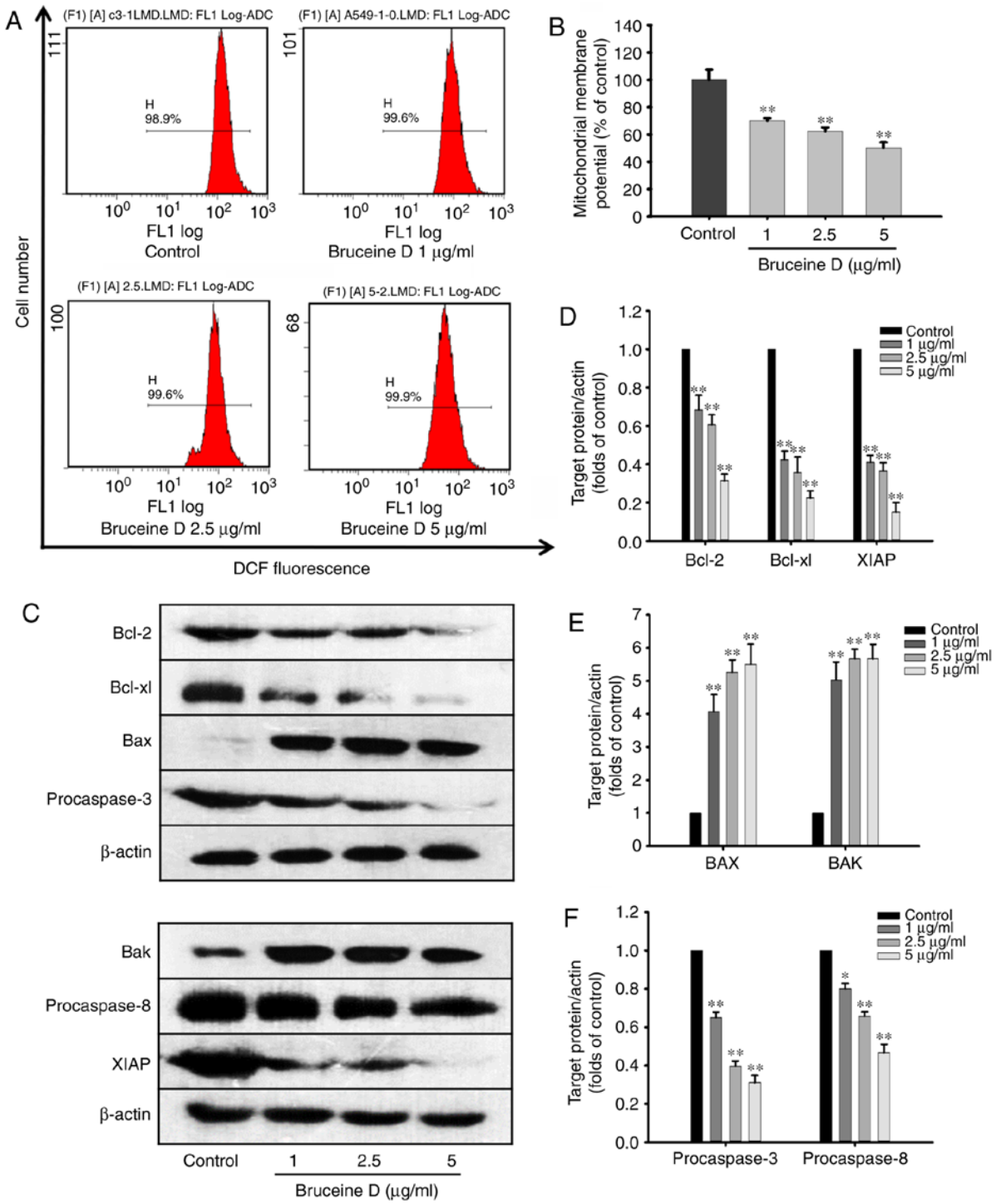

Figure 6. Effects of bruceine D on mitochondrial function and mitochondrial-associated apoptotic proteins in A549 NSCLC cells. (A) Flow cytometric analysis of Δψm as estimated by Rhodamine 123 intensity. (B) Column bar graph of cell fluorescence for Rhodamine 123. Data are presented as the mean ± standard error of the mean of three independent experiments. Statistical analyses were performed using Fisher's least significant difference test. (C) Effects of bruceine D on the expression of mitochondrial apoptosis pathway-associated proteins (Bcl-2, Bcl-xl, XIAP, Bax, Bak, pro-caspase-3 and pro-caspase-8) in A549 cells. (D) Densitometry analysis of the protein expression levels of Bcl-2, Bcl-xl and XIAP. (E) Densitometry analysis of the protein expression levels of Bax and Bak. (F) Densitometry analysis of the protein expression levels of pro-caspase-3 and pro-caspase-8. β-actin was used as the protein loading control. *P<0.05, **P<0.01 vs. control. NSCLC, non-small-cell lung cancer; XIAP, X-linked inhibitor of apoptosis.

Caspases are known to be activated during apoptosis in numerous cell types and play key roles in the initiation and execution of mitochondria-mediated apoptosis (34). Pro-caspase-3 activation is a hallmark of apoptotic induction through both the extrinsic and intrinsic apoptotic pathways. In the extrinsic pathway, pro-caspase-3 is activated by pro-caspase-8 (37). In the present study, western blotting demonstrated that bruceine D simultaneously decreased the protein expression of pro-caspase-3 and pro-caspase-8, suggesting that a mitochondria-associated pathway is involved in the induction of apoptosis by bruceine D. However, further investigations are required to improve our understanding of the detailed underlying mechanism.

The results of the present demonstrate that bruceine D exerts its anti-NSCLC effects at least partially via triggering the mitochondrial ROS-mediated death signaling pathway. bruceine D appears to be a potent antiproliferative and apoptosis-inducing component of *B. javanica*, and may contribute to the anticancer activity of this medicinal herb. These findings may improve our understanding of the molecular mechanisms underlying the anticancer properties of bruceine D, further elucidate the pharmacodynamics of bruceine D, and support the ethnomedical application of *B. javanica* and its preparations against NSCLC. This may provide a basis for future *in vivo* studies and the potential clinical application of bruceine D in the treatment of lung cancer. Further research is required to identify other pivotal signaling pathways induced by bruceine D in A549 NSCLC cells. Future animal studies are also warranted to fully elucidate the value of bruceine D as a treatment option for NSCLC.

Acknowledgements

Not applicable.

Funding

The present study was supported by the Natural Science Foundation of Shenzhen University General Hospital (grant nos. SUGH2018QD070 and SUGH2018QD035), the Youth Innovative Talents Project of Colleges and Universities of Guangdong Province (grant no. 2018KQNCX216), the Science and Technology Planning Project of Guangdong Province, China (grant no. 2017A050506044), the Science and Technology Planning Project of Guangzhou, Guangdong, China (grant no. 201704030028), the Natural Science Foundation of Guangdong Province, China (grant no. 2018A030313408), the Science and Technology Research Project of Guangdong Provincial Hospital of Chinese Medicine (grant no. YN2018ZD02), the National Natural Science Foundation of China (grant no. 81503458), the Science and Technology Planning Project of Guangdong Province, China (grant nos. 2016A020226036 and 2017B030314166), the General Research Fund from the Research Grants Council of Hong Kong (grant no. 469912), the Science and Technology Planning Project of Guangdong Province (grant no. 2017B030314166), the Characteristic Cultivation Program for Subject Research of Guangzhou University of Chinese Medicine (grant no. XKP2019007), and the Key Program for Subject Research of Guangzhou University of Chinese Medicine (grant no. XK2018016 and XK2019002).

Availability of data and materials

The datasets generated and analyzed during the present study are available from the corresponding author on reasonable request.

Authors' contributions

YLX, JNC, ZRS, ZXL and XBY were involved in developing the concept and design of the study, and are guarantors of the integrity of the study. JHX and ZQL performed the experiments, prepared and revised the manuscript. XHZ and YFX were responsible for the literature review and assisted with data analysis. QL and SPI performed the experiments and revised the manuscript. All authors have read and approved the final version of the manuscript submitted for publication.

Ethics approval and consent to participate

Not applicable.

Patient consent for publication

Not applicable.

Competing interests

The authors declare that they have no competing interests.

References

1. Segal RL, Miller KD and Jemal A: Cancer statistics, 2018. CA Cancer J Clin 68: 7-30, 2018.
2. Huang CY, Ju DT, Chang CF, Muralidhar Reddy P and Velmurugan BK: A review on the effects of current chemotherapy drugs and natural agents in treating non-small-cell lung cancer. Biomedicine (Taipei) 7: 23, 2017.
3. Newman DJ and Cragg GM: Natural products as sources of new drugs from 1981 to 2014. J Nat Prod 79: 629-661, 2016.
4. Zhao L, Li C, Zhang Y, Wen Q and Ren D: Phytochemical and biological activities of an anticancer plant medicine: *Brucea javanica*. Anticancer Agents Med Chem 14: 440-458, 2014.
5. Lichota A and Gwozdzinski K: Anticancer activity of natural compounds from plant and marine environment. Int J Mol Sci 19: pii: E3533, 2018.
6. Lau ST, Lin ZX, Liao Y, Zhao M, Cheng CH and Leung PS: Brucein D induces apoptosis in pancreatic adenocarcinoma cell line PANC-1 through the activation of p38-mitogen activated protein kinase. Cancer Lett 281: 42-52, 2009.
7. Lau ST, Lin ZX and Leung PS: Role of reactive oxygen species in Brucein D-mediated p38-mitogen-activated protein kinase and nuclear factor kappaB signalling pathways in human pancreatic adenocarcinoma cells. Br J Cancer 102: 583-593, 2010.
8. Lai ZQ, Ip SP, Liao HJ, Lu Z, Xie JH, Su ZR, Chen YL, Xian YF, Leung PS and Lin ZX: Bruceine D, a naturally occurring tetracyclic triterpene quassinoid, induces apoptosis in pancreatic cancer through ROS-associated PI3K/Akt signaling pathway. Front Pharmacol 22: 936, 2017.
9. Lau ST, Lin ZX, Zhao M and Leung PS: *Brucea javanica* fruit induces cytotoxicity and apoptosis in pancreatic adenocarcinoma cell lines. Phytother Res 22: 477-486, 2008.
10. Liu L, Lin ZX, Leung PS, Chen LH, Zhao M and Liang J: Involvement of the mitochondrial pathway in bruceine D-induced apoptosis in Capan-2 human pancreatic adenocarcinoma cells. Int J Mol Med 30: 93-99, 2012.
11. Chinese Pharmacopoeia Commission (CP): Pharmacopoeia of the People's Republic of China. China Medical Science Press, Beijing, pp254-255, 2015.
12. Liu JH, Qin JJ, Jin HZ, Hu XJ, Chen M, Shen YH, Yan SK and Zhang WD: A new triterpenoid from *Brucea javanica*. Arch Pharm Res 32: 661-666, 2009.
13. Lee KH, Imakura Y, Sumida Y, Wu RY, Hall IH and Huang HC: Antitumor agents. 33. Isolation and structural elucidation of bruceoside-A and -B, novel antileukemic quassinoid glycosides, and brucein-D and -E from *Brucea javanica*. J Org Chem 44: 2180-2185, 1979.
14. Ablat A, Halabi MF, Mohamad J, Hasnan MH, Hazni H, Teh SH, Shilpi JA, Mohamed Z and Awang K: Antidiabetic effects of *Brucea javanica* seeds in type 2 diabetic rats. BMC Complement Altern Med 17: 94, 2017.
15. Zhou L, Wei E, Zhou B, Bi G, Gao L, Zhang T, Huang J, Wei Y and Ge B: Antiproliferative benefit of curcumol on human bladder cancer cells via inactivating EZH2 effector. Biomed Pharmacother 104: 798-805, 2018.

16. Xian YF, Lin ZX, Zhao M, Mao QQ, Ip SP and Che CT: Uncaria rhynchophylla ameliorates cognitive deficits induced by D-galactose in mice. Planta Med 77: 1-7, 2011.
17. Otto T and Sicinski P: Cell cycle proteins as promising targets in cancer therapy. Nat Rev Cancer 17: 93-115, 2017.
18. Redza-Dutordoir M and Averill-Bates DA: Activation of apoptosis signalling pathways by reactive oxygen species. Biochim Biophys Acta 1863: 2977-2992, 2016.
19. Zorova LD, Popkov VA, Plotnikov EY, Silachev DN, Pevzner IB, Jankauskas SS, Babenko VA, Zorov SD, Balakireva AV, Juhaszova M, *et al*: Mitochondrial membrane potential. Anal Biochem 552: 50-59, 2018.
20. Hata AN, Engelman JA and Faber AC: The BCL-2 family: Key mediators of the apoptotic response to targeted anticancer therapeutics. Cancer Discov 5: 475-487, 2015.
21. Pfeffer CM and Singh ATK: Apoptosis: A target for anticancer therapy. Int J Mol Sci 19: pii E448, 2018.
22. Cheng Z, Yuan X, Qu Y, Li X, Wu G, Li C, Zu X, Yang N, Ke X, Zhou J, *et al*: Bruceine D inhibits hepatocellular carcinoma growth by targeting β-catenin/jagged1 pathways. Cancer Lett 403: 195-205, 2017.
23. Zhang JY, Lin MT, Tung HY, Tang SL, Yi T, Zhang YZ, Tang YN, Zhao ZZ and Chen HB: Bruceine D induces apoptosis in human chronic myeloid leukemia K562 cells via mitochondrial pathway. Am J Cancer Res 6: 819-826, 2016.
24. Wei SC and Yang J: Forcing through tumor metastasis: The interplay between tissue rigidity and epithelial-mesenchymal transition. Trends Cell Biol 26: 111-120, 2016.
25. Cerella C, Grandjenette C, Dicato M and Diederich M: Roles of apoptosis and cellular senescence in cancer and aging. Curr Drug Targets 17: 405-415, 2016.
26. Rather RA and Bhagat M: Cancer chemoprevention and piperine: Molecular mechanisms and therapeutic opportunities. Front Cell Dev Biol 6: 10, 2018.
27. Kumari S, Badana AK, G MM, G S and Malla R: Reactive oxygen species: A key constituent in cancer survival. Biomark Insights 13: 1177271918755391, 2018.
28. Tan SWS, Lee QY, Wong BSE, Cai Y and Baeg GH: Redox homeostasis plays important roles in the maintenance of the drosophila testis germline stem cells. Stem Cell Reports 9: 342-354, 2017.
29. Couto N, Wood J and Barber J: The role of glutathione reductase and related enzymes on cellular redox homoeostasis network. Free Radic Biol Med 95: 27-42, 2016.
30. Traverso N, Ricciarelli R, Nitti M, Marengo B, Furfaro AL, Pronzato MA, Marinari UM and Domenicotti C: Role of glutathione in cancer progression and chemoresistance. Oxid Med Cell Longev 2013: 972913, 2013.
31. Georgieva E, Ivanova D, Zhelev Z, Bakalova R, Gulubova M and Aoki I: Mitochondrial dysfunction and redox imbalance as a diagnostic marker of 'free radical diseases'. Anticancer Res 37: 5373-5381, 2017.
32. Kim YM, Youn SW, Sudhahar V, Das A, Chandhri R, Cuervo Grajal H, Kweon J, Leanhart S, He L, Toth PT, *et al*: Redox regulation of mitochondrial fission protein Drp1 by protein disulfide isomerase limits endothelial senescence. Cell Rep 23: 3565-3578, 2018.
33. Baig S, Seevasant I, Mohamad J, Mukheem A, Huri HZ and Kamarul T: Potential of apoptotic pathway-targeted cancer therapeutic research: Where do we stand? Cell Death Dis 7: e2058, 2016.
34. Siddiqui WA, Ahad A and Ahsan H: The mystery of BCL2 family: Bcl-2 proteins and apoptosis: An update. Arch Toxicol 89: 289-317, 2015.
35. Kale J, Osterlund EJ and Andrews DW: BCL-2 family proteins: Changing partners in the dance towards death. Cell Death Differ 25: 65-80, 2018.
36. Castelli G, Pelosi E and Testa U: Emerging therapies for acute myelogenus leukemia patients targeting apoptosis and mitochondrial metabolism. Cancers (Basel) 11: pii: E260, 2019.
37. Kiraz Y, Adan A, Kartal Yandim M and Baran Y: Major apoptotic mechanisms and genes involved in apoptosis. Tumour Biol 37: 8471-8486, 2016.